LUND UNIVERSITY

Rotational Cars Generation Through A Multiple Four-color Interaction

Aldén, Marcus; Bengtsson, Per-Erik; Edner, H

Link to publication

Rotational CARS generation through a multiple four-color interaction

Marcus Aldén, Per-Erik Bengtsson, and Hans Edner

A novel technique for the generation of single-pulse rotational CARS spectra is presented and demonstrated in gas flows and flames. The technique is based on a multiple four-color interaction, where the rotational energies are excited with two photons of different frequencies from a broadband dye laser, and by coupling to a third photon from a frequency-doubled Nd:YAG laser a rotational CARS photon is created. An interesting feature of the technique is the possibility of simultaneously generating both a rotational and vibrational CARS spectrum using a double-folded BOXCARS arrangement. This technique is demonstrated on N_2 molecules.

I. Introduction

With the advent of a tunable laser source in the mid-1960s several new analytical techniques were created with applications in different areas, e.g., chemistry, biology, and physics. One of the most promising techniqes is coherent anti-Stokes Raman scattering (CARS), which is a nonlinear optical technique involving a four-wave mixing process. The great potential of CARS for analytical purposes was soon realized, and, especially in combustion diagnostics, its coherent nature and considerable signal strength were big advantages. Pioneering work in applying CARS to combustion analyses was carried out in the mid-1970s by Taran and co-workers.[1,2] The technique was later developed to include single-shot capabilities[3] and to yield highly spatially resolved measurements through the introduction of the BOXCARS concept.[4] These achievements made it possible to use CARS even in very hostile environments such as sooty flames,[5] turbulent combustors,[6] and large oil- and coal-fired furnaces.[7,8]

In a CARS experiment the signal beam is generated spatially very close to the primary laser beams. When probing energy vibrations, which for most molecules are between 1000 and 4000 cm^{-1}, the problem of spectrally isolating the CARS beam can be easily solved by using dichroic mirrors and interference filters. All work referred to so far has utilized vibrational CARS.

However, when using CARS for probing pure rotational energy splittings, which are normally <300 cm^{-1}, considerable difficulties are encountered in spectral discrimination for the much stronger laser beams. In the first reported rotational CARS experiments this problem was not too severe since hydrogen molecules were studied,[9] which due to their low molecular weight have a very large rotational constant and, therefore, a rotational spectrum clearly separated from the laser beams used. In that work the $J = 3 \rightarrow 5$ rotational transition with a Raman shift of 1033 cm^{-1} was studied. Later work reported studies of lower rotational Raman shifts using a four-color scheme[10] and a nonphase-matched arrangement.[11] The breakthrough in examining very low rotational Raman shifts with CARS was made by introduction of the folded BOXCARS technique,[12] where the CARS beam is spatially isolated from the primary laser beams. This technique was later used for cold gas and flame temperature measurements.[13,14]

There are several reasons why rotational CARS may provide a complement to, or even a better choice than, ordinary vibrational CARS, especially at lower temperatures. The rotational lines are much easier to resolve than the piled-up rotational lines in a vibrational Q-branch which must be evaluated by elaborate computer codes for temperature determination. The rotational Raman linewidths are in general narrower and the cross sections are larger than those corresponding to vibrational CARS, which leads to higher signal intensity. Another advantage with rotational CARS is that one single dye can be used to measure simultaneously several different species. The largest drawback with rotational CARS is the fact that the population difference factor, inherent in all CARS processes, decreases the signal intensity at higher temperatures more severely than in vibrational CARS.

Until today most rotational CARS experiments have been performed using a Nd:YAG-based laser system, which has meant that the frequency-doubled Nd:YAG beam at 532 nm is used together with a dye laser utilizing coumarin as the dye. However, this dye suffers from several drawbacks such as lower efficiency, much faster degradation, and larger spectral intensity variations than, e.g., rhodamine dyes. The latter factor limits the temperature accuracy in single-shot rotational CARS experiments as pointed out by Zheng et al.[14]

In this paper we present an alternative way of producing rotational CARS spectra. An arbitrary broadband dye laser is used so that two photons from two identical dye laser beams couple pairwise to a third photon from the 532-nm beam to generate a rotational CARS photon in the spectral vicinity of 532 nm. This technique is similar to the dual-broadband CARS technique demonstrated on vibrational transitions for multiple species detection by Eckbreth and Anderson.[15] One potential advantage with these techniques is a smoothing effect on the dye laser noise due to the fact that many frequency combinations drive each individual Raman resonance, which also was experimentally verified in this paper. An additional advantage with this technique is that with proper phase-matching conditions it is possible to generate simultaneously rotational and vibrational CARS spectra with very little additional experimental complexity. This approach could be of use in the diagnostics of turbulent media with highly fluctuating temperatures. In this case vibrational CARS may be used for measurements in the hot parts, while rotational CARS is used to probe the cooler parts.

In Sec. II.A. is a brief description of rotational CARS. The presentation and general features of the new concept for the generation of rotational CARS spectra are discussed in Sec. II.B. In Sec. III the experimental setup and measurements with pure rotational CARS will be described, while in Sec. IV the simultaneous rotational and vibrational CARS concept will be described and exemplified. Finally, in Sec. V a discussion and conclusions will be presented.

II. Rotational CARS

A. Conventional Rotational CARS

As in vibrational CARS, the rotational CARS beam is generated when one of two laser beams $\omega_{green} (= \omega_g)$ and $\omega_{red-shifted} (= \omega_r)$ is tuned so that the frequency difference $\omega_g - \omega_r$ is equal to a Raman-allowed transition, in this case a rotational transition. When the phase-matching conditions are fulfilled, the intensity in the CARS beam at frequency $\omega_{g,CARS} = 2\omega_g - \omega_r$ is given by

$$I(\omega_{g,CARS}) \sim |\chi^{(3)}|^2 I_g^2 I_r, \qquad (1)$$

where $\chi^{(3)}$ is the third-order nonlinear susceptibility, I_g and I_r are the laser intensities in the two primary laser beams. Since the electronic background susceptibility is negligible in a pure rotational experiment[16] we have that

$$\chi^{(3)} = \sum_j \chi_j^r, \qquad (2)$$

where χ_j^r is the complex resonant susceptibility for the jth Raman transition given by

$$\chi_j^r \sim \frac{N\Delta_j g_j}{\Gamma_j} \left(\frac{d\sigma}{d\Omega}\right)_j \frac{i}{[1 + i\Delta\omega_j/(\Gamma_j/2)]} = \chi_{0j}^r \left(\frac{i}{1 + ix}\right), \qquad (3)$$

where N is the total number density, Δ_j is the population difference factor between the levels of the jth Raman transition, $(d\sigma/d\Omega)_j$ is the differential spontaneous Raman cross section, and $\Delta\omega_j$ is the laser detuning frequency from the jth Raman resonance at ω_R, i.e., $\Delta\omega_j = \omega_R - (\omega_g - \omega_r)$ and g_j is a weighting factor dependent on the nuclear spin. It is evident from Eqs. (1)–(3) that the CARS signal for a single resonance is given by

$$I(\omega_{g,CARS}) \sim (\chi_0^r)^2 \frac{1}{1 + x^2}, \qquad (4)$$

which is a Lorentzian with a full width at half-maximum (FWHM) of Γ, the homogeneous rotational Raman linewidth. The most temperature-dependent factor in Eq. (3) as a function of J-quantum numbers is the population difference factor Δ. In rotational CARS for a $J \rightarrow J + 2$ transition this factor is given by [12]

$$\Delta_j = \frac{(2J + 1)}{Q} \left\{ \exp\left[-J(J + 1)\frac{hcB}{kT}\right] - \exp\left[-(J + 2)(J + 3)\frac{hcB}{kT}\right] \right\}, \qquad (5)$$

where Q is the rotational partition function.

To generate a rotational CARS spectrum one has to include the difference in linewidth Γ for different J quantum numbers and temperatures. We have used the J- and T-dependent linewidth of N_2 from Hall,[17] where an analytical form for Γ in the vibrational Q branch is given. Following the argument in Ref. 18, this formula was used rather than extrapolating the Γ values given by Jammu et al.[19] to higher J-quantum numbers and temperatures, as is normally done. It is also necessary to take into account differences in the weighting factor g_j for odd and even J-quantum numbers. Since the nitrogen atom has a nuclear spin equal to one, the weighting factors for even and odd J-quantum numbers are 6 and 3, respectively. This means that there is a factor of 4 difference in intensity between consecutive J values due to the quadratic CARS dependence.

B. New Concept for Rotational CARS Generation

The concept for rotational CARS implemented in this work was pointed out by Yuratich[20] and is related to the dual-broadband CARS approach introduced by Eckbreth and Anderson.[15] In the latter work it is shown how two independent broadband Stokes sources can be arranged together with a narrowband pump laser to generate vibrational CARS signals from several species simultaneously. Each dye laser mixes separately with the pump laser in a normal CARS process, while there is also a mixing process for Raman
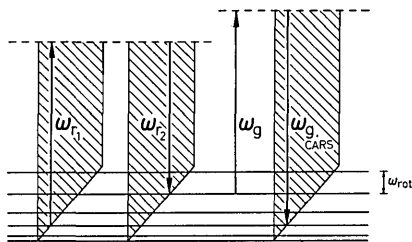
Fig. 1. Energy-level diagram for generation of rotational CARS spectra using a multiple four-color interaction process.

resonances matching the frequency difference of the two broadband sources. Thus it is possible to simultaneously generate signals from, e.g., CO_2, H_2O, and N_2, where N_2 is the dual-broadband component. In this paper we adopt a similar process to probe much smaller Raman shifts, such as rotational transitions, using frequency differences within one single dye.

The principle of this new method for rotational CARS generation is illustrated in Fig. 1. Assuming a Nd:YAG-based laser system the frequency-doubled Nd:YAG laser at 532 nm ω_g and a broadband red dye ω_r are employed. $\omega_{r,1}$ and $\omega_{r,2}$ are two frequencies of many possible pairs with a frequency difference matching a rotational transition in a molecule. The excitation induced by $\omega_{r,1}$ and $\omega_{r,2}$ is then scattered off by the narrowband ω_g beam, resulting in a CARS beam $\omega_{g,CARS}$ at $\omega_g + \omega_{r,1} - \omega_{r,2}$. The spectral resolution of the CARS signal is determined by the linewidth of ω_g and the slit function of the spectrometer. Both CARS and CSRS (coherent Stokes Raman scattering) signals will be generated on different sides of the ω_g frequency, since phase-matching conditions are almost fulfilled for both processes simultaneously. Simultaneous generation of CARS and CSRS signals has earlier been observed using a broadband green dye covering both sides of 532 nm.[21,22] The CARS and CSRS spectra contain identical information about the rotational levels, and several of the presented spectra here are in fact CSRS spectra. However, for simplicity, they are also referred to as CARS spectra.

A single-broadband dye can cover several J numbers in the rotational CARS spectra. However, there will be a decrease in signal toward higher Raman shifts due to the limited spectral bandwidth of the dye. This bandwidth function can easily be calculated assuming Gaussian dye profiles. Since it arises from a convolution of two Gaussian profiles the resulting FWHM for a dye will be $\sqrt{2} \cdot \Delta\sigma$, where $\Delta\sigma$ is the FWHM of the dye itself. This dependence was also experimentally verified by using the nonresonant signal from a species with no rotational structure. The achieved rotational CARS spectra must of course be compensated for this function before temperature interpretation can be performed. By calculating the function for different dyes with the same total output power and a specific ratio in $\Delta\sigma$, it is apparent that the function show the same ratio in intensity at zero shift and in FWHM. The optimal choice of dye depends on how high J numbers are to be

probed, and both $\Delta\sigma$ and output power have to be taken into account. Since the signal has a quadratic dependence on the dye laser intensity, an efficient rhodamine dye is favored at lower rotational shifts, whereas, e.g., the very broad dye DCM is preferable at large Raman shifts ($\gtrsim 200$ cm^{-1}).

Different phase-matching schemes are possible, but since the CARS frequency is close to the ω_g frequency, the CARS beam should be spatially isolated from the ω_g beam. The simplest solution is to use planar BOXCARS phase-matching with two ω_r beams and one ω_g beam. The CARS beam is then generated in a direction close to one of the ω_r beams but free from the ω_g beam and can easily be isolated with beam dumps and dichroic mirrors before entering the spectrometer. This is to be compared to the conventional technique of generating broadband rotational CARS spectra with a broad green dye in the spectral vicinity of ω_g. In the latter case it is necessary to use a folded BOXCARS scheme, often combined with polarization techniques, to isolate the CARS beam sufficiently. Folded BOXCARS can also be employed in the new concept and a double-folded BOXCARS scheme with two ω_r, and two ω_g beams can be arranged to generate rotational and vibrational CARS spectra simultaneously. ω_r is then chosen so that $\omega_g - \omega_r$ covers a vibrational resonance. If there is a strong resonance this will also be seen as background in the rotational CARS spectrum. This is due to the fact that the vibrational excitation induced by ω_g and ω_r can be scattered off by the broadband ω_r beam, resulting in a diffuse background around ω_g. This effect and the concept for simultaneous generation of rotational and vibrational CARS will be further discussed in Sec. IV.

III. Experimental

The experimental setup used in the pure rotational CARS measurement is shown in Fig. 2. A Quanta-Ray DCR-1 Nd:YAG laser is frequency-doubled with a KD*P type II crystal and used to pump a Quanta-Ray PDL-1 dye laser with an oscillator followed by a preamplifier and longitudinally pumped final amplifier. The dye laser, with a rhodamine or DCM dye, was made broad band by replacing the grating with a mirror. The power in this ω_r beam was between 25 and 50 mJ depending on which dye was used. Since in our approach the dye-laser energy exhibits a quadratic
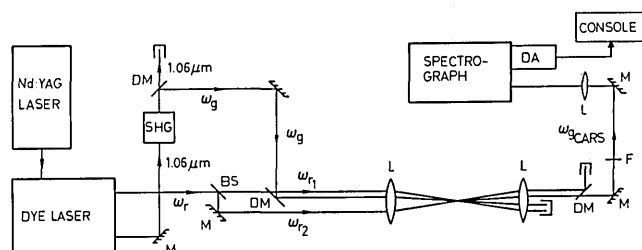

Fig. 2. Experimental setup for generation of rotational CARS spectra: DM, dichroic mirror; BS, beam splitter; M, mirror; L, lens; F, cutoff filter; DA, diode array; SHG, second harmonic generator.

CARS power dependence, the dye laser was pumped with all available green laser radiation from the Nd:YAG laser. The green beam at 532 nm is, therefore, produced by frequency-doubling of the residual IR beam in a second doubling crystal yielding ~20 mJ at 532 nm, the ω_g beam. The green beam and the two dye laser beams were aligned in a planar BOXCARS configuration with one of the red beams and the green beam almost superimposed, focused, and crossed together with the second red beam with a crossing angle of ~3°. The broadband rotational CARS beam was generated from the common focal point and followed the direction of the dye laser beam $\omega_{r,2}$, which meant that the CARS beam could be spectrally isolated with a dichroic mirror. The signal beam was focused onto the entrance slit of a home-built 1-m spectrograph with a dispersion of 2.7 Å/mm in the fourth order. The detection system consisted of a PARC OMA III unit with an intensified and gateable 1420 detector head and a 1460 main frame. The experimental setup described above is advantageous compared with the folded BOXCARS setup normally used in rotational CARS experiments, because the correct positions for lenses, apertures, and narrow slits could be more easily found, since the CARS beam is generated almost collinearly with the red dye laser beam $\omega_{r,2}$.

Measurements were performed on an open gas flow containing pure N_2 or O_2. The peak intensity and spectral profiles of the generated rotational CARS spectra were compared for different dyes, rhodamine 610, rhodamine 640, kiton red, and DCM, with the strongest signal at room temperature obtained with kiton red. Figure 3 shows a typical single-shot recording from O_2 at 300 K with a spectral resolution of 2.0 cm^{-1}. The spectrum is not corrected for the dye laser bandwidth. At room temperatures the CARS beam had to be attenuated before entering the spectrometer in order not to saturate the detector. The maximum single-shot signal for N_2 with an ~3 times lower cross section than O_2, was 2000 counts with a 1% transmission neutral density filter.

We did not in the present work make any experimental comparison between the new approach and the conventional one for the generation of rotational CARS spectra with regard to signal intensity and noise. However, Figs. 4(a) and (b) show portions of the normalized spectral profiles of coumarin 500 and rhodamine 640, respectively, captured in three individual shots. The advantage of using a rhodamine dye regarding spectral noise is apparent, as discussed earlier. Figure 4(c) also shows three normalized single-shot recordings of the nonresonant rotational background CARS spectrum with rhodamine 640 as the dye. This was achieved by focusing the laser beams inside a high-pressure cell filled with CH_4 at 8 atm. The average of 100 shots of this kind could be used to correct the rotational CARS spectra. Methane was used since it has no Raman-active rotational resonances.

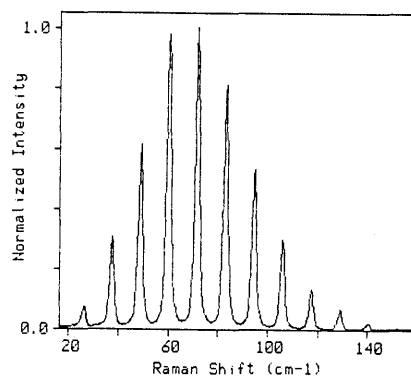To establish the smoothing effect on the noise in the rotational CARS spectra caused by multiple-frequen-

Fig. 3. Single-shot rotational CARS spectrum from O_2 at 300 K.
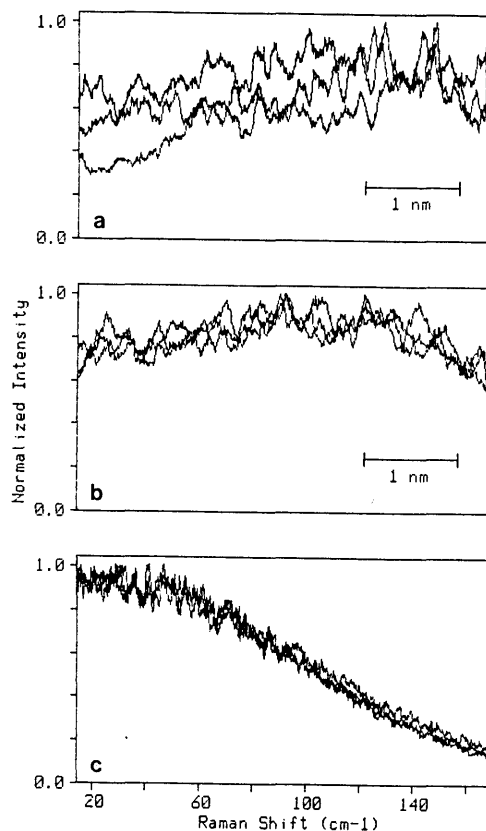

Fig. 4. Three normalized single-shot spectral distributions for (a) coumarin 500, (b) rhodamine 640, and (c) the rotational CARS background using rhodamine 640.

cy combinations (mfc), comparisons were made between the noise in the nonresonant CARS spectra with the mfc and the conventional vibrational CARS techniques when using rhodamine 640 as dye. The noise was determined by analyzing single-pulse nonresonant spectra divided by a 100-pulse average spectrum. The evaluation was made for single diodes (~0.25 cm^{-1}) over a region of 50 cm^{-1}. The data were corrected for detector shot noise, assuming that the pulse-to-pulse variation in the nonresonant CARS signal and the

detector shot noise were statistically uncorrelated. The resulting mean noise for twenty pulses with the conventional technique was 9.6% (single standard deviation), while a similar evaluation of the dye laser noise yielded 4.9%. These figures are in good accordance with other measurements utilizing a multimode pump laser.[23,24] The noise in the rotational CARS setup was in the same way determined to be 4.7%, thus a factor of ~2 reduction compared to the noise in conventional CARS. The corresponding noise utilizing other dyes and dye combinations was not investigated in the present work. Preliminary experiments indicate that the rotational CARS noise is even lower for, e.g., rhodamine 610, but no comparison with a conventional CARS setup was made here.

Measurements were also performed on a $CH_4/O_2/N_2$ flame at a temperature of ~1700 K. Here the broader DCM dye was employed, and the pixels of the diode array were grouped in the readout sequence to improve the SNR. This lowered the spectral resolution, but the lines were still fully resolved. The SNR for a single shot was about one in the present setup, so signal averaging had to be employed. However, after improvements single-shot measurements should also be possible at these temperatures.

IV. Simultaneous Rotational and Vibrational CARS Generation

A big advantage with the current technique for the generation of rotational CARS spectra is that with minor changes in the experimental setup it is possible to generate simultaneously a vibrational CARS spectrum. This is achieved by a double-folded BOXCARS arrangement, as indicated in Fig. 5, where $\omega_{r,1}$, $\omega_{r,2}$, and
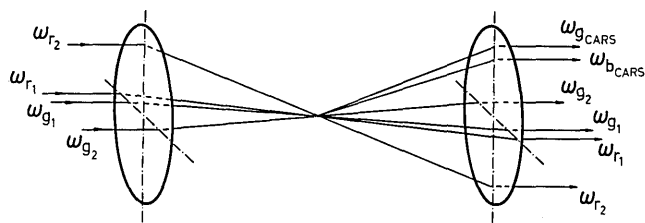
Fig. 5. Phase-matching conditions for simultaneous generation of rotational and vibrational CARS spectra.

$\omega_{g,2}$ produce a rotational CARS beam at $\omega_{g,CARS}$ in a similar way as that described in Sec. II. $\omega_{r,2}$, $\omega_{r,1}$, and $\omega_{g,2}$ could at the same time be used as in a normal vibrational folded BOXCARS setup to produce a vibrational CARS beam at $\omega_{b,CARS}$. Of course, the condition $\omega_{g,1} - \omega_{r,2} = \omega_R$, where ω_R is the vibrational Raman shift for the studied molecule, has to be fulfilled as usual. The two CARS beams generated almost on top of each other could then be focused on the spectrograph and detected as described in Sec. III. The setup is obtained by first optimizing the vibrational CARS signal according to the planar BOXCARS scheme with $\omega_{g,1}$, $\omega_{g,2}$, and $\omega_{r,1}$. When these three beams give a maximum CARS signal, the fourth beam, $\omega_{r,2}$, is introduced, and a vibrational folded BOXCARS beam is created by $\omega_{g,1}$, $\omega_{g,2}$, and $\omega_{r,2}$. When both of these schemes are optimized, phase-matching will also be fulfilled for small shifts in the rotational folded BOXCARS arrangement.

To demonstrate the possibility of simultaneously generating and detecting a rotational and vibrational CARS spectrum, a much smaller spectrograph, a Jarrell/Ash with a 600-r/mm grating yielding a dispersion of 60 Å/mm, was used. Figure 6 shows the simultaneously generated N_2 vibrational CARS spectrum at 473 nm and the corresponding rotational CARS and CSRS spectra in the spectral vicinity of scattered light from the laser beam at 532 nm. In this experiment rhodamine 640 was used, with its spectral peak intensity tuned to 607 nm, as is also shown in Fig. 6. The dye was wavelength-tuned by increasing the dye-oscillator concentration. The rotational and vibrational CARS intensities are normalized in the figure, since a comparison between the two processes is very dependent on the laser intensity. As described above, we have in these experiments optimized the rotational CARS intensity in that the dye laser intensity was optimized.

Simultaneously generated rotational and vibrational CARS spectra were also studied at different temperatures, 300 K < T < 700 K, with clear single-shot capabilities. To achieve higher spectral resolution, the 1-m spectrograph was employed. Thus the different rotational and vibrational CARS spectra, although generated at the same time, were detected consecutively by changing the grating position in the spectrograph. One way to detect simultaneously high resolved rotational and vibrational CARS spectra is to use a ruled grating in different orders. However, a more practical solution may be to use the $\omega_{r,1}$, $\omega_{g,1}$, and
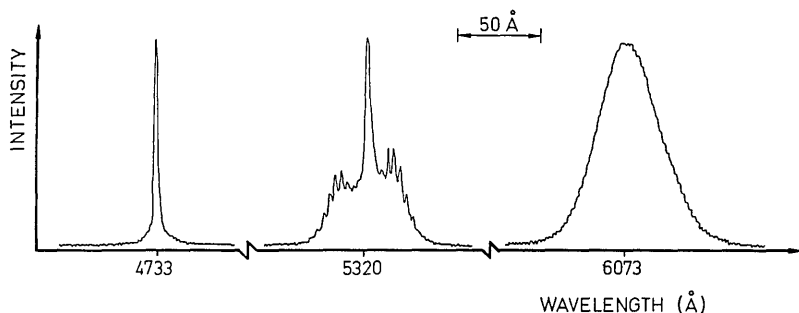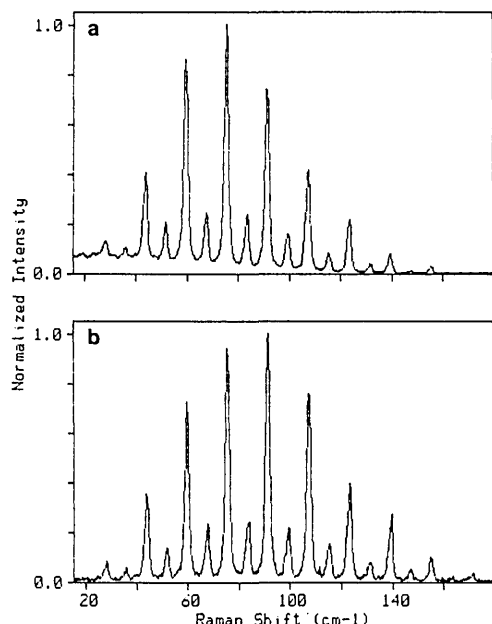
Fig. 6. Simultaneously detected vibrational CARS spectrum at 473 nm and rotational CARS and CSRS spectra around 532 nm. The dye laser profile at 607 nm is also shown.

Fig. 7. Rotational CARS spectra of N_2 molecules captured by a single laser pulse using (a) rhodamine 640 and (b) DCM, illustrating the background CARS signal when using the rhodamine dye. The effect of dye laser bandwidth is also apparent.
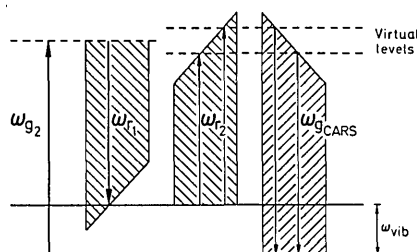

Fig. 8. Energy-level diagram for generation of a broadband background CARS signal.

$\omega_{g,2}$ beams in planar BOXCARS for vibrational CARS and the $\omega_{r,1}$, $\omega_{r,2}$, and $\omega_{g,2}$ beams in folded BOXCARS for rotational CARS and thus create the two CARS beams spatially separated. The two beams could then be detected by two separate spectrograph/diode array systems.

During this series of experiments it was realized that when using a dye at ω_r which gives a vibrational Raman resonance, i.e., $\omega_g - \omega_r = \omega_R$, a background appears in the rotational spectra. This is clearly illustrated in Fig. 7, which shows a single-shot rotational CARS spectrum from N_2 obtained using the resonant dye rhodamine 640, shown in Fig. 7(a), while when using the nonresonant dye DCM a background-free spectrum was achieved as shown in Fig. 7(b). This background was also very clearly shown when probing methane, with a vibrational Raman shift around 3000 cm^{-1}, and DCM as dye. The background is due to a four-wave mixing process illustrated in Fig. 8. Here

the vibrational splitting is driven by one green and one red photon. This vibration is then coupled to a second red photon, and since the red beam is broadband this type of CARS beam spectrally mirrors the dye laser profile in the spectral vicinity of 532 nm. The exact spectral position of this CARS beam depends on where in the broadband dye laser profile the vibrational Raman resonance is situated. If the dye laser has its peak on the resonance, the broadband distribution will peak at exactly 532 nm. This background will also be present in a pure rotational setup if a vibrational resonant dye is utilized. For the question of how this background influences the accuracy in a temperature determination, two things have to be considered. First, since the background essentially spectrally mirrors the broadband dye laser an additional noise factor will be present. However, by looking at Fig. 7(a) it is apparent that the background is <10% of the peak rotational CARS intensity, and since the dye laser noise is ~5% (single standard deviation) the resulting noise in the rotational CARS spectra should be considerably <1% and thus gives a minor contribution to a temperature determination. The second thing that has to be considered is that the ratio between background and rotational CARS intensity is temperature dependent. Since the background CARS signal depends on the laser beams involved in the rotational CARS process it is not possible to obtain the background-free CARS signal by subtraction. However, it seems quite possible to achieve a background-free spectrum by simply interpolating between the base lines of adjacent rotational peaks.

V. Conclusions

Although the rotational CARS intensity has been calculated and experimentally verified to be of the same order as a vibrational CARS spectrum at room temperature,[14,18] comparatively few papers have described applications of rotational CARS. One reason, until the introduction of the folded BOXCARS technique, was the difficulty in rejecting the very strong background from the pump laser. When a dye laser beam was also used as a pump beam, problems arose because of broad superfluorescence from the dye. Today, when using fixed-frequency solid-state lasers and folded BOXCARS, the problems have arisen from the poor dye pumping efficiency, short dye lifetime, difficulties in wavelength-tuning broadband dye, and large spectral irregularities of the dye when pumping with a 3 × Nd:YAG pump laser and coumarin dye. The technique presented in this paper reduces all these problems to the same level as encountered in vibrational CARS, since with this technique an arbitrary yellow-red dye can be used, e.g., the very stable and highly efficient rhodamine 6G.

One potential problem with the technique was the signal intensity. We have not made a comparison with a conventional rotational Raman setup, but we did compare the peak rotational CARS intensity with the peak vibrational intensity for N_2 at room temperature with two optimized systems. Optimized in this sense

means that the laser beam having a quadratic CARS power dependence was optimized, i.e., for rotational CARS the dye laser and in vibrational CARS the 532-nm beam. The results indicate that, within experimental error, the two intensities were of the same order at room temperature. The rotational CARS signal intensity can be further increased through improvements in our experimental setup. Tests after the measurements showed that a better blazed grating could increase the rotational signal 4 times. Furthermore, the most efficient dye, rhodamine 6G, was not employed in the present measurements due to the fact that the correct dichroics were not available. Also the fact that the multiple-frequency combinations gives a noise reduction in the rotational CARS spectrum is of great interest. This fact has recently also been theoretically verified.[25] More detailed investigations concerning the influence of dye laser bandwidth on the CARS noise and comparison between our technique, conventional rotational CARS, and vibrational CARS for temperature accuracy will be further investigated.

The problem with this technique is at high temperatures, where the rotational intensity peak has moved to high J-quantum numbers. The problem arises because the available dye laser power is low, especially for dyes like rhodamines and kiton red. The best dye here is DCM, which is very broad. Our results indicate that this dye, although not as efficient as the others, was the only one that could be used for flame measurements. However, neither the effect of binary dye combinations nor the effect of solvent and concentration was investigated in the present work.

The possibility of simultaneously generating rotational and vibrational CARS spectra seems to be an attractive technique, when one wants to make single-shot temperature measurements in, e.g., turbulent flames, explosions, or sparks. In these processes the temperatures must be measured in terms of a probability distribution function (pdf). A problem with using a conventional CARS technique here is that the intensity difference between a hot and a cold CARS spectrum is much larger than the dynamic range of the optical multichannel analyzers used in broadband CARS. This fact has necessitated the use of a multiarrangement of beam splitters[26] or a special beam splitter inside the spectrograph.[27] In the simultaneous vibrational/rotational CARS approach the vibrational CARS spectrum could be used for high-temperature measurements ($\gtrsim 1\,100$ K), where the strength of the hot band is great enough for accurate temperature evaluation, while the rotational CARS spectra would be used for measurements at lower temperatures.

We believe that the proposed technique for generating rotational CARS spectra should increase the role of rotational CARS in combustion diagnostics. One field where rotational CARS is advantageous, compared with vibrational CARS, is at high pressures because of the more widely spaced rotational transitions which would avoid the complication of motional narrowing and also at low temperature combustion. Thus areas in which rotational CARS might be of interest are

studies in internal combustion engines and in gas turbines.

Note added in proof: After submission of this paper we learned of the recent letter by Eckbreth and Anderson,[28] who also have adopted the new technique of generating pure rotational CARS and CSRS spectra. Their conclusions are in good accordance with the ones presented in this paper.

References

1. P. R. Regnier and J. P. E. Taran, "On the Possibility of Measuring Gas Concentrations by Stimulated Anti-Stokes Scattering," Appl. Phys. Lett. 23, 240 (1973).
2. P. R. Regnier, F. Moya, and J. P. E. Taran, "Gas Concentration Measurement by Coherent Raman Anti-Stokes Scattering," AIAA J. 12, 826 (1974).
3. W. B. Roh, P. W. Schreiber, and J. P. E. Taran, "Single-Pulse Coherent Anti-Stokes Raman Scattering," Appl. Phys. Lett. 29, 174 (1976).
4. A. C. Eckbreth, "BOXCARS: Crossed-Beam Phase-Matched CARS Generation in Gases," Appl. Phys. Lett. 32, 421 (1978).
5. A. C. Eckbreth, "CARS Thermometry in Practical Combustors," Combust. Flame 39, 133 (1980).
6. D. A. Greenhalgh, F. M. Porter, and W. A. England, "The Application of Coherent Anti-Stokes Raman Scattering to Turbulent Combustion Thermometry," Combust. Flame 49, 171 (1983).
7. M. Aldén and S. Wallin, "CARS Experiments in a Full-Scale (10 × 10 m) Industrial Coal Furnace," Appl. Opt. 24, 3434 (1985).
8. E. J. Beiting, "Multiplex CARS Temperature Measurements in a Coal-Fired MHD Environment," Appl. Opt. 25, 1684 (1986).
9. J. J. Barrett, "Generation of Coherent Anti-Stokes Rotational Raman Radiation in Hydrogen Gas," Appl. Phys. Lett. 29, 722 (1976).
10. I. R. Beattie, T. R. Gilson, and D. A. Greenhalgh, "Low Frequency Anti-Stokes Raman Spectroscopy of Air," Nature London 276, 378 (1978).
11. L. P. Goss, J. W. Fleming, and A. B. Harvey, "Pure Rotational Coherent Anti-Stokes Raman Scattering of Simple Gases," Opt. Lett. 5, 345 (1980).
12. J. A. Shirley, R. J. Hall, and A. C. Eckbreth, "Folded BOXCARS for Rotational Raman Studies," Opt. Lett. 5, 380 (1980); Y. Prior, "Three-Dimensional Phase Matching in Four-Wave Mixing," Appl. Opt. 19, 1741 (1980).
13. D. V. Murphy and R. K. Chang, "Single-Pulse Broadband Rotational Coherent Anti-Stokes Raman-Scattering Thermometry of Cold N_2 Gas," Opt. Lett. 6, 233 (1981).
14. J. Zheng, J. B. Snow, D. V. Murphy, A. Leipertz, R. K. Chang, and R. L. Farrow, "Experimental Comparison of Broadband Rotational Coherent Anti-Stokes Raman Scattering (CARS) and Broadband Vibrational CARS in a Flame," Opt. Lett. 9, 341 (1984).
15. A. C. Eckbreth and T. J. Anderson, "Dual Broadband CARS for Simultaneous, Multiple Species Measurements," Appl. Opt. 24, 2731 (1985); A. C. Eckbreth and T. J. Anderson, "Dual Broadband USED CARS," Appl. Opt. 25, 1534 (1986).

16. L. M. Roland and W. A. Steele, "Intensities in Pure Rotational CARS of Air," J. Chem. Phys. **73**, 5919 (1980).
17. R. J. Hall, "Pressure-Broadened Linewidths for N_2 Coherent Anti-Stokes Raman Spectroscopy Thermometry," Appl. Spectrosc. **34**, 700 (1980).
18. R. J. Hall and A. C. Eckbreth, "Coherent Anti-Stokes Raman Spectroscopy (CARS): Application to Combustion Diagnostics," in *Laser Applications, Vol. 5*, J. F. Ready and R. K. Erf, Eds. (Academic, New York, 1984).
19. K. S. Jammu, G. S. St. John, and H. L. Welsh, "Pressure Broadening of the Rotational Raman Lines of Some Simple Gases," Can. J. Phys. **44**, 797 (1966).
20. M. A. Yuratich, "Effects of Laser Linewidth on Coherent Anti-Stokes Raman Spectroscopy," Mol. Phys. **38**, 625 (1979).
21. M. Aldén, H. Edner, and S. Svanberg, "Coherent Anti-Stokes Raman Spectroscopy (CARS) Applied in Combustion Probing," Phys. Scr. **27**, 29 (1983).
22. J. B. Zheng, A. Leipertz, J. B. Snow, and R. K. Chang, "Simultaneous Observation of Rotational Coherent Stokes Raman Scat-
tering and Coherent Anti-Stokes Raman Scattering in Air and Nitrogen," Opt. Lett. **8**, 350 (1983).
23. D. R. Snelling, R. A. Sawchuk, and R. E. Mueller, "Single Pulse CARS Noise: A Comparison Between Single-Mode and Multimode Pump Lasers," Appl. Opt. **24**, 2771 (1985).
24. D. A. Greenhalgh and S. T. Whittley, "Mode Noise in Broadband CARS Spectroscopy," Appl. Opt. **24**, 907 (1985).
25. S. Kröll, M. Aldén, T. Berglind, and R. J. Hall, to be published.
26. L. P. Goss, D. D. Trump, B. G. MacDonald, and G. L. Switzer, "10-Hz Coherent Anti-Stokes Raman Spectroscopy Apparatus for Turbulent Combustion Studies," Rev. Sci. Instrum. **54**, 563 (1983).
27. A. C. Eckbreth, "Optical Splitter for Dynamic Range Enhancement of Optical Multichannel Detectors," Appl. Opt. **22**, 2118 (1983).
28. A. C. Eckbreth and T. J. Anderson, "Simultaneous Rotational Coherent Anti-Stokes Raman Spectroscopy and Coherent Stokes Raman Spectroscopy with Arbitrary Pump-Stokes Spectral Separation," Opt. Lett. **11**, 496 (1986).

Fabrication of an x-ray imaging detector

An x-ray detector array that could yield a mosaic image of an object emitting in the 1–30-keV range could be fabricated from an n-doped silicon wafer. The detector is an improved version of the device described in "X-Ray Detector for 1 to 30 keV" (GSC-12682), *NASA Tech Briefs*, **7**, No. 3 (Spring, 1983), page 248.

In the proposed fabrication technique, thin walls of diffused n^+ dopant would divide the wafer into pixels of rectangular cross section, each containing a central electrode of thermally migrated p-type metal. This pnn^+ arrangement would reduce the leakage current by preventing the transistor action caused by the pnp structure of the earlier version.

The n-type conductivity in the silicon wafer would be produced by doping it lightly with phosphorus. For 1–30 keV x-rays the wafer thickness would be $\sim$1.27 mm. Relatively thin layers ($\sim$2000 Å thick) of silicon dioxide would be formed on the wafer surfaces by exposing it to steam and oxygen while its temperature is maintained at $\sim$1000°C.

In the first step in the pixel formation, a photoresist mask is applied to the upper surface of the wafer to delineate the walls. The surface is etched in a buffered hydrofluoric acid solution to remove selectively the upper silicon dioxide layer in a pattern defining the pixel walls.

A laser is used to drill circular openings, $\sim$0.025 mm in diameter, centered every 0.05 mm along the etched pattern and passing perpendicularly completely through the wafer. The wafer, placed in a furnace at 1100°C, would then be exposed to a phosphorus gas dopant ($POCl_3$ in a mixture of gaseous nitrogen and oxygen) for a time sufficient to assure diffusion of the dopant atoms to a distance of 0.025 mm from the axis of each opening, the phosphorus atoms diffusing from adjacent openings thus coming into contact to produce continuous walls of n^+ atoms.

Metallic strips, preferably aluminum, would then be evaporated over the exposed wall areas of the top surface to contact the diffused phosphorus, forming the interconnected configuration shown in Fig. 8. A similar array of aluminum strips, contacting the diffused phosphorus at the openings, would be produced evaporatively on the lower wafer surface.

To locate the thin aluminum electrodes centered in each pixel, a photoresist mask with openings at the pixel centers is applied to the upper wafer surface. The masked wafer is etched with hydrofluoric acid to expose the silicon in the center. Then, after the photoresist mask is stripped using hot chromic acid and the wafer rinsed clean, aluminum is evaporated over the top wafer surface. A second photoresist mask is then used to protect the aluminum film at the future electrode sites while the rest of the film is etched with phosphoric

acid. After the second mask is stripped with chromic acid and the wafer rinsed clean, the lower surface of the wafer is heated to $\sim$1150°C, while the upper surface is kept slightly cooler at $\sim$1100°C. The resulting thermal gradient causes the aluminum deposited in the etched opening on the cooler surface to form the central electrodes by diffusing completely through the wafer to the opposite surface. The aluminum strips connecting the n^+-diffused regions also diffuse through the wafer to form aluminum walls between the pixels.

Since this rapid diffusion allows little time for lateral diffusion, the cross section of each electrode is small compared with the cross section of each pixel, thereby minimizing the probability of x-rays impinging directly on the central electrodes. To enhance the spatial resolution of an x-ray image, the horizontal cross section of each pixel is kept small: the separation between the central electrodes of adjacent pixels is $\sim$1 mm.
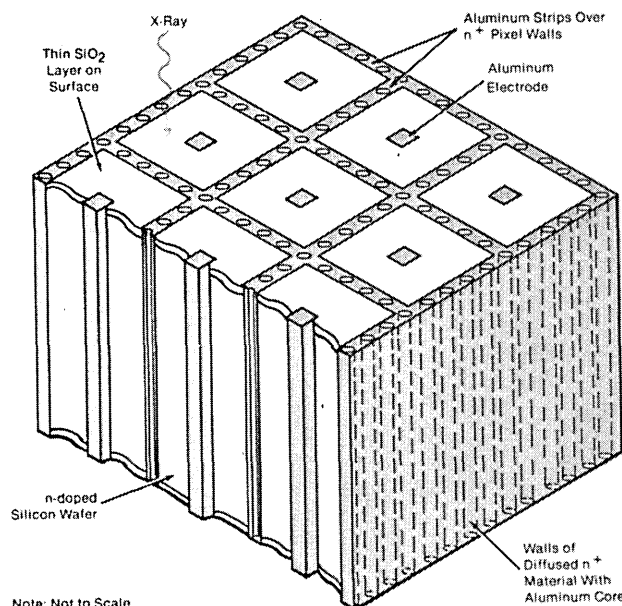

Fig. 8. X-ray detector array fabricated from a single silicon wafer consists of pixels of n-doped silicon separated by n^+ walls and containing aluminum (p) electrodes.